The Journal of Immunology

Dendritic Cells Require the NF-κB2 Pathway for Cross-Presentation of Soluble Antigens

Evan F. Lind, Cory L. Ahonen, Anna Wasiuk, Yoko Kosaka, Burkhard Becher, Kathy A. Bennett and Randolph J. Noelle

J Immunol 2008; 181:354-363; ;
doi: 10.4049/jimmunol.181.1.354
http://www.jimmunol.org/content/181/1/354

The Journal of Immunology is published twice each month by
The American Association of Immunologists, Inc.,
1451 Rockville Pike, Suite 650, Rockville, MD 20852

Print ISSN: 0022-1767 Online ISSN: 1550-6606.

Dendritic Cells Require the NF-κB2 Pathway for Cross-Presentation of Soluble Antigens[1]

Evan F. Lind,* Cory L. Ahonen,* Anna Wasiuk,* Yoko Kosaka,* Burkhard Becher,† Kathy A. Bennett,* and Randolph J. Noelle[2]*

NF-κB-inducing kinase (NIK) is responsible for activation of the non-canonical p100 processing pathway of NF-κB activation. This kinase has been shown to be critical for activation of this pathway after signaling through several TNF family members including CD40. The functional importance of this pathway in CD40 and TLR-induced dendritic cell (DC) differentiation was studied in vivo in the alymphoplasia (Aly) mouse. The Aly mouse expresses a mutant NIK molecule that prohibits the induction of the non-canonical pathway. We show that while MHC class II presentation and in vivo migration of Aly DCs is intact, these cells are unable to cross-prime CD8$^+$ T cells to exogenous Ag. Gene expression array analysis of DCs matured in vivo indicates multiple defects in Ag processing pathways after maturation and provide a global view of the genes that are regulated by the NF-κB2 pathway in DCs. These experiments indicate a possible role for NIK in mediating cross-priming of soluble Ag. In addition, our findings explain the profound immune unresponsiveness of the Aly mouse. ***The Journal of Immunology,*** **2008, 181: 354–363.**

Central to the immunologic function of dendritic cells (DC)[3] is their maturation induced by TNF family members. TNF-α, CD154, and RANKL are all TNF family members that induce DC maturation. Common to the signaling of many TNFRs is the activation of the canonical and non-canonical NF-κB pathways. Although the role of the canonical NF-κB pathway has been extensively studied in DC, the role of the non-canonical pathway has not yet been fully resolved. NF-κB-inducing kinase (NIK) is a serine/threonine kinase that was identified as a potential activating kinase in the NF-κB pathway (1). Later it was shown that NIK is not required for activation of the canonical NF-κB pathway (2) but rather is involved in a second non-canonical NF-κB pathway (3). Activation of this non-canonical pathway results in phosphorylation of IKKα by NIK. This results in ubiquitination and partial proteasomal degradation of the p100 NF-κB2 precursor protein releasing active p52 and p52/RelB dimers that then target transcriptional activation of responsive genes (4, 5). Activation of this pathway has been shown to occur by signaling through several TNFR family members including lymphotoxin β receptor (6), BAFF receptor (7), CD40 (8), and others.

Mice that bear spontaneous or engineered mutations in the NIK gene (2, 9) have been used to study the role of NIK in immune function. These mutant mice provide the unique opportunity to study the role of the non-canonical pathway in DC maturation in vivo. The alymphoplasia (Aly) mouse bears a spontaneous single point mutation in the NIK gene resulting in an inability of NIK to interact with the IKK complex (9–12). Several groups have studied the requirement for specific NF-κB subunits in DC development and function. These studies all focus on mice or cells lacking a specific member or members of the NF-κB family (13–17). To study specifically the role for the NF-κB2 pathway in DC function, we conducted the studies presented here in the Aly mouse. The data shows that the NIK defect incapacitates the activation of the NF-κB2 pathway in DCs as measured by the inability of Aly DCs (DC^{Aly}) to translocate p52 to the nucleus in response to CD40 engagement. This observation was followed by a series of in vivo studies to investigate the breadth and depth of DC deficiencies imposed by this selective impairment in NF-κB2 activation. The studies reveal a series of very well defined DC functions that are controlled by the NF-κB2 pathway. Furthermore, transcriptional profiling of heterozygous DCs (DC^{WT}) and homozygous mutant DC (DC^{Aly}) matured in vivo provide a global view of the gene expression regulated by the non-canonical and canonical pathways in DCs in vivo.

Materials and Methods

Mice

Aly mice were obtained from CLEA, Japan. All Aly mice were bred and housed at the pathogen-free animal facility at Dartmouth Medical School. TAP1−/−, OT1, and OT2 mice were purchased from The Jackson Laboratory. Animal experiments were performed in accordance with institutional guidelines.

Abs and cell lines

The CD8OVA CD8$^+$ T cell hybridoma was a gift of Dr. Brent Berwin (Dartmouth Medical School, Dartmouth, NH) with the permission of Dr. Clifford V. Harding (Case Western Reserve University, Cleveland, OH). Abs specific to CD45.1, CD86, CD8, H-2D^b, and B220 were all purchased from BioLegend. Abs specific to CD80, 41BB-L, CD150, CD70, IA/IE, CD103, and IFN-γ were all purchased from eBiosciences. OVA tetramer H-2K^b SIINFEKL PE was purchased from Beckman Coulter. Anti-DEC 205 was purchased from Serotec. Anti-CD40 and anti-CD4 were conjugated in house. Anti-CD11c clone HL3 (PE and FITC) were a gift from Dr. Leo Lefrancois (University of Connecticut Medical Center, Farmington, CT). Agonistic anti-CD40 clone FGK4.5 was purchased from Bio Express. Endotoxin content of the anti-CD40 Ab was <1 EU/mg as determined by

*Department of Microbiology and Immunology, Dartmouth Medical School and the Norris Cotton Cancer Center, Lebanon, NH 03756; and †Department of Neurology, Neuroimmunology Unit, University of Zurich, Zurich, Switzerland

Received for publication June 11, 2007. Accepted for publication April 25, 2008.

The costs of publication of this article were defrayed in part by the payment of page charges. This article must therefore be hereby marked *advertisement* in accordance with 18 U.S.C. Section 1734 solely to indicate this fact.

[1] This work was supported by National Institutes of Health Grant CA09143 to R.N.

[2] Address correspondence and reprint requests to Dr. Randolph J. Noelle, Department of Microbiology and Immunology, Norris Cotton Cancer Center, Dartmouth Hitchcock Medical Center, Dartmouth Medical School, 1 Medical Center Drive, Lebanon, NH 03756. E-mail address: rjn@dartmouth.edu

[3] Abbreviations used in this paper: DC, dendritic cell; NIK, NF-κB-inducing kinase; Aly, alymphoplasia.

a quantitative chromogenic *limulus* amebocyte lysate kit (QCL 1000; Cambrex).

DC isolation

Mouse spleens were enzymatically digested with a mixture of Liberase/DNase I (Roche Applied Sciences) solution. DCs were isolated via MACS $CD11c^+$ bead selection (Miltenyi Biotec). Post-isolation purity was determined by staining cells with a different clone of anti-CD11c Ab, HL3, and anti-MHC class II Abs. For gene arrays, bead purification was followed by FACS sorting to high purity (98% or greater) for expression of both CD11c and MHC class II.

DC adoptive transfers and OT1 expansion in TAP1−/− mice

On day −1, 5×10^6 OT1 $CD8^+$ CFSE-labeled cells were injected i.v. into TAP1−/− recipients. Cells were isolated via negative magnetic bead selection for CD8 (Miltenyi Biotec). Twenty four hours later, mice received 5×10^5 DCs i.v. from either wild-type (WT) or Aly mice that were pulsed with whole OVA protein (25 mg/ml; Sigma-Aldrich), pulsed with SIINFEKL peptide (1 mg/ml), or unpulsed for 3 h in vitro. At the time of DC injection, mice received 25 μg of LPS and 100 μg of anti-CD40 to mature DCs. Spleens were isolated 72 h later and stained with anti-CD8 and OVA H-$2K^b$ tetramer for analysis.

OT2 expansion in WT or Aly mice

WT or Aly mice received 1×10^6 CFSE-labeled OT2 cells purified by negative magnetic selection. Twenty four hours later they received 25 μg of LPS to mature the DCs and 2 mg of whole OVA, or no treatment as control. At indicated days, mice were sacrificed and OT2 expansion and IFN-γ production was assessed. For intracellular IFN-γ staining, spleen cells were incubated with PMA/ionomycin and monensin (eBioscience) for 2 h at 37°C. Cells were then stained for the OT2 congenic marker CD45.1 and CD4, followed by fixation/permeabilization using the Cyto perm/fix kit (BD Biosciences) and staining for IFN-γ for 30 min at 4°C.

Western blotting

For NF-κB2, cytoplasmic extracts were made by hypotonic lysis for 15 min in 10 mM HEPES (pH 7.6), 1 mM EDTA, 0.1 mM EGTA, 10 mM KCl, 1 mM DTT, with leupeptin, aprotinin, pepstatin, and PMSF present. In the last 5 min, IGEPAL (Sigma-Aldrich) was added to a final concentration of 0.6%. Nuclei were then pelleted and resuspended in 20 mM HEPES (pH 7.6), 0.2 mM EDTA, 0.1 mM EGTA, 25% glycerol, 0.42 M NaCl, 1 mM DTT, in the presence of protease inhibitors. Debris was removed by centrifugation and samples were denatured in 2× SDS buffer with 2-ME. Proteins were detected by rabbit polyclonal anti-NF-κB2 (p100/p52), provided by Dr. Steven C. Ley (National Institute for Medical Research, Mill Hill, London, U.K.). Equal nuclear loading was assured by blotting for SAM68 (Santa Cruz Biotechnology).

Ag uptake

For Alexa Fluor 488 LDL, Alexa Fluor 488 latex beads and DQ OVA uptake, DCs were isolated from spleens of Aly or WT mice by Miltenyi CD11c magnetic beads ($CD11c^+$ isolated population typically >95% pure). DCs were cultured for 2 h at 37°C in RPMI 1640 with either Alexa Fluor 488 AcLDL or Alexa Fluor 488 latex beads or for 6 h with indicated concentration of DQ OVA. After 4 h, cells were washed and analyzed on a BD FACScan measuring FL1 (530/30 BP filter) fluorescent signal. To measure OVA-Alexa Fluor 488 uptake in vitro, DCs were isolated as mentioned above and cultured for 2.5 h with 10 μg/ml OVA-Alexa Fluor 488 at either 37°C or 4°C. For OVA-Alexa Fluor 488 uptake in vivo, mice were injected i.v. with 100 μg of OVA-Alexa Fluor 488 or unlabeled OVA as a control, splenic DCs were analyzed 24 h later. In both cases, cells were stained with Abs specific to CD11c and CD8. Alexa Fluor 488 fluorescence was then measured on populations by gating on $CD11c^+$ cells, and then gating on either $CD8^+$ or $CD8^-$ subpopulations.

Histology

Spleens were frozen in OCT (Sakura Finetek USA), over dry ice ethanol bath and stored at –70°C until use. Tissue was sectioned at 5 μm on a cryostat. Slides were fixed in 4°C acetone, dried and rehydrated in PBS. Sections were stained with anti-CD4 FITC, anti-CD11c PE, and anti-B220 APC. Images were captured using a Zeiss LSM 510 confocal microscope.

Cross-priming of $CD8^+$ T cells to soluble Ag in vivo

WT or Aly mice were treated i.p. with 25 μg of LPS (055:B5; Sigma-Aldrich), 100 μg of agonistic anti-CD40 (clone FGK4.5), and 2 mg of whole OVA protein. Six days later, spleen cells were stained with anti-CD8 PE, and OVA H-$2K^b$ tetramer APC. Representative of three experiments, $n = 3$ mice per experiment. In vivo cytotoxicity assay was conducted as described previously (18). Target cells were injected into Aly or WT mice, 5 days after challenge with 500 μg of whole OVA protein, 50 μg of anti-CD40, and 200 μg of TLR7 agonist S-27609 (3M Pharmaceuticals).

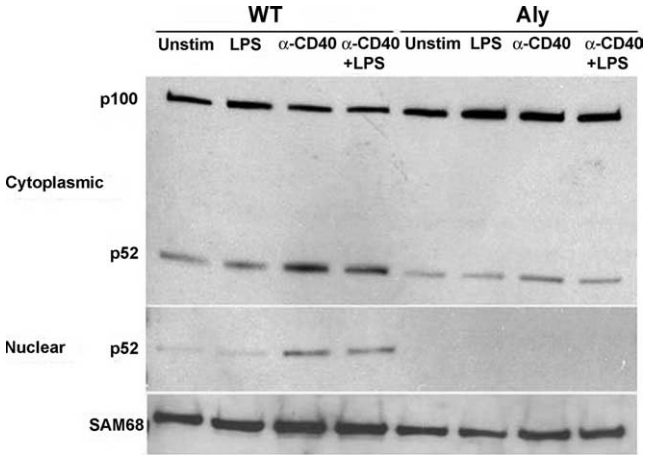

FIGURE 1. DC^{aly} fail to translocate p52 to the nucleus after CD40 engagement. DC were placed in culture for 18 h with either 500 ng/ml LPS or 10 μg/ml agonistic anti-CD40 Ab or both. Nuclear and cytoplasmic fractions were separated and blots were detected with Abs that detect both p100 and processed p52. SAM68 was used as a nuclear loading control.

Gene array

Mice were treated in vivo for 6 h with both 25 μg of LPS and 100 μg of agonistic anti-CD40. Each experiment had 3 mice per group. RNA was pooled per each experiment. Experiment was performed three separate times per group. Statistical differences were decided based on *t* test of raw chip signals between groups $p < 0.05$ for statistically different genes (see Fig. 7), or $p > 0.05$ for genes not different. Genes included in list have a fold change of 1.5 or more above un-stimulated and an average chip signal of 100 minimum in the stimulated groups. Heat map image derived from normalization of signals after statistics for display purposes, image made using MeV software by Institute for Genomic Research (TIGR). Microarray data are available from the National Center for Biotechnology Information Gene Expression Omnibus under accession no. GSE7219.

Results

DC^{Aly} fail to translocate p52 to the nucleus in response to CD40 engagement

Initial studies were designed to evaluate the biochemical role of NIK in murine DCs triggered by innate and/or adaptive signals. Proteolytic processing of NF-κB p100 to p52 is tightly regulated, and is a measurement of non-canonical NF-κB activity. Following triggering by agonistic anti-CD40 and/or LPS, the magnitude of cellular p52 expression and the nuclear translocation of p52 was measured and used as an index of NF-κB2 activation. Purified $CD11c^+$ splenic DCs from WT (DC^{WT}) and Aly (DC^{Aly}) mice were cultured overnight with LPS, anti-CD40 Ab, or both. As shown in Fig. 1, triggering via CD40 in the presence or absence of LPS in DC^{WT} increases the abundance of cytoplasmic p52 as well as the nuclear translocation of p52. Activation of DC^{Aly} with anti-CD40 and/or LPS failed to induce either an increase in p52 in the cytoplasm or nuclear translocation. Therefore, similar to B cells (8), triggering via CD40 and not TLR in DCs activates the non-canonical NF-κB2 cascade. However, DC^{Aly} triggered with either anti-CD40 and/or LPS failed to activate the NF-κB2 cascade.

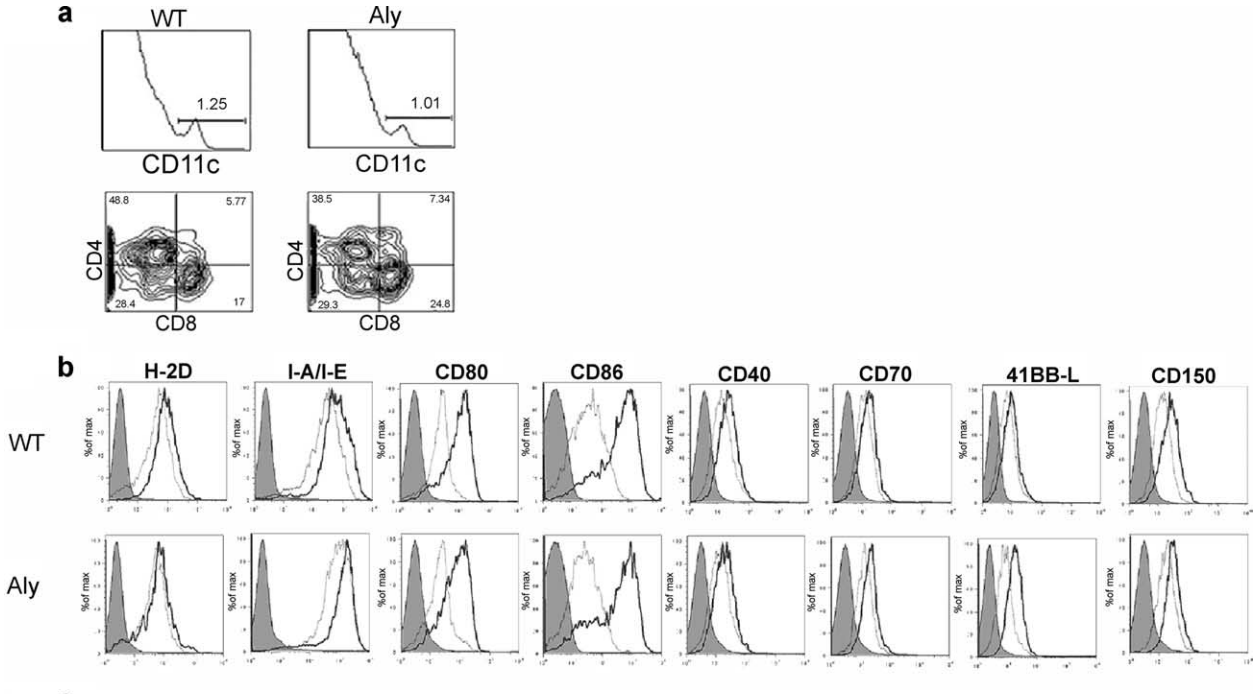

c

Gene	Fold Increse WT	Aly	Gene	Fold Increase WT	Aly
IL2ra	36.0	18.8	Ikbk3	43.2	30.9
IL4ra	18.1	26.5	Nfkb2	10.5	9.8
IL10ra	2.0	2.0	Foxp4	7.7	10.3
			Spic	6.2	8.0
CD80	18.1	25.4	Traf1	4.1	3.4
CD40	13.8	15.5	Traf6	2.1	2.6
CD99	7.2	4.1	Jak1	3.5	1.9
CD151	1.9	2.3	Jak2	3.0	1.8
CD223	9.1	25.8	Jak3	4.0	2.2
Tnfrsf1b TNF-α R	2.7	2.5	Stat3	5.8	3.9
Tnfrsf19l (RELT)	2.1	1.2	Socs1	3.9	3.9
			Map4k4	7.3	8.5
Bcl2l1	10.6	15.9	Mapk6	3.0	1.8
Bcl7c	5.0	6.2	Junb	3.4	2.2
Bcl9l	4.9	4.0	Mapk6	5.3	3.8
Bcl2l11	5.8	3.7	Map3k14 (NIK)	3.3	6.5
Bcl2l14	4.3	2.3	Ikbkb	3.2	2.8
Mcl1	2.1	1.4	Foxp1	2.6	1.5
Serpina3g	2.4	1.8	Ripk1	2.2	1.2
Bcl2a1a	2.3	2.0	Akt3	8.6	7.4
Fadd	2.0	1.6			
Pdcd4	4.5	6.6	B2m	4.4	2.6
Pcdcd1lg2	3.2	9.9	Tapbp	3.7	2.5
			Psmb10	3.3	2.7
Cxcl1	3.9	3.8	Psme2	2.9	2.4
			Lamp2	2.2	1.3
			Tap1	3.5	2.0
			Psma4	1.7	0.9

FIGURE 2. Phenotypic distribution and in vivo maturation of Aly DCs. *a*, Frequency and distribution of Aly DCs in vivo. Spleens were digested with DNase and Liberase and then stained for CD11c, CD4 and CD8. Fig. 2a shows distribution of $CD4^+$ vs $CD8^+$ populations after gating on CD11c+ cells. *b*, In vivo maturation of DCs. WT or Aly mice were treated for 18 h with LPS and anti-CD40 Ab. After treatment, spleens were digested as in *a* and stained with Abs specific to indicated markers. All histograms gated on CD11c+ populations. Light lines represent untreated levels. Dark lines represent levels after treatment. Shaded histograms represent isotype controls. *c*, Gene array profiling of WT or Aly DCs matured in vivo. Mice were treated for 6 h with both LPS and anti-CD40. DCs were then isolated to high purity and RNA was isolated for gene array profiling. Displayed are genes which respond to stimuli in a similar manner in both Aly and WT DCs. Fold increase represents the average fold induction of listed gene over unstimulated. Numbers represent average chip signal induction, which were statistically induced over untreated by *t* test $p < 0.05$, that were also induced in Aly DCs. Signals are averages from three individual experiments, three mice per group pooled RNA.

The Aly mutation does not alter the development of DC subsets or their ability to up-regulate the expression of selected cell surface molecules

NF-κB subunit defects have been shown to affect DC subset development (17, 19). Phenotypic multiparameter analysis of Aly or WT littermates for CD11c, CD4 vs CD8 revealed that the subsets of DCs present in either the homozygous mutant and heterozygous littermates were indistinguishable (Fig. 2*a*). Recent studies into DC function have implicated DC subsets expressing both CD8 and DEC205 (20) and CD103 (21) as the cells responsible for

cross-priming. We undertook a separate series of studies to verify that those subsets were in fact present in the Aly mouse. There were no measurable differences between Aly and WT mice in the frequency of CD103 or DEC 205 positive cell populations (data not shown). Studies were also designed to evaluate whether the ability to up-regulate the expression of cell surface molecules on DCs was altered by the Aly mutation. After in vivo maturation of DCs, by treating mice for 18 h with combined TLR/CD40 agonists, staining was performed to observe baseline untreated levels and in vivo-induced up-regulation of cell surface molecules on DC^{WT} or DC^{Aly}. The data shown in Fig. 2*b* indicate that there are no overt differences in the up-regulation of MHC class I or II in WT or mutant mice. Costimulatory molecule expression and up-regulation of CD80/86, CD40, CD70, 41BB-L, or CD150 are indistinguishable between DC^{WT} and DC^{Aly}. This observation is in agreement with recent work (22) that observed maturation of Aly DC in vitro by measuring levels of CD86, CD40, and MHC class I.

Maturational status of DC^{Aly} after stimulation in vivo with TLR/anti-CD40 was further investigated by gene array profiling. Six hours after stimulation, splenic DCs were isolated to high purity, and RNA was extracted and analyzed by whole mouse genome Affymetrix array. As can be seen in Fig. 2*c*, there are a series of genes that are up-regulated in both the DC^{WT} and DC^{Aly} after maturation with TLR/anti-CD40. Included in this list are many components of signaling cascades such as NF-κB2 and NIK, perhaps indicating that players in the non-canonical NF-κB pathway are regulated in a positive way during maturation. The fact that many early events in DC maturation appear normal in the Aly mouse is not surprising due to the specific nature of the mutation in NIK regulating the non-canonical NF-κB pathway.

The Aly mutation specifically impairs cross-priming

One of the unique features of matured DCs is their ability to cross-prime $CD8^+$ T cells. To evaluate the role of NIK in cross-priming, WT or Aly mice were immunized with soluble OVA protein, anti-CD40, and TLR agonist. Administration of whole OVA with anti-CD40 and TLR agonist has been shown previously to induce robust cross-priming of endogenous $CD8^+$ T cells in vivo (18). Following immunization of WT and Aly mice, the frequency of endogenous OVA-specific $CD8^+$ T cells was measured using OVA-H-2^b tetramer. OVA-specific cytolytic activity was also measured using an in vivo cytotoxicity assay. Immunization of WT mice with OVA, using either a TLR4 or TLR7 agonist together with anti-CD40, induced robust expansion of OVA-specific $CD8^+$ T cells. In the WT mice, the tetramer-positive cells represented 3–7% of the $CD8^+$ T cells (Fig. 3, *a* and *c*). In addition, high levels of in vivo OVA-specific CTL activity were observed (Fig. 3, *b* and *d*). In contrast, immunization of Aly mice with OVA, anti-CD40, and TLR4 or TLR7 agonist, did not induce the appearance of OVA-specific $CD8^+$ T cells or enhance OVA-specific cytolytic activities. Hence, using an immunization regime that induces extremely high frequencies of Ag-specific CTLs, the Aly mutation ablates cross-priming in vivo. To verify that the functional $CD8^+$ T cell responses we see in the WT mouse are due to processing of whole OVA protein rather than direct exchange of any possible contaminating peptide fragments present in our OVA preparation, we performed a similar experiment using TAP1−/− mice as vaccine recipients (data not shown). The failure of TAP1−/− mice to respond indicates that processing of the OVA protein is required in our vaccine protocol and that the impact of any possible contaminating peptide fragments is negligible in this model. It is interesting to note that recently it has been shown that RelB is involved in cross-priming by DCs (13). RelB has been shown to preferentially act as a dimer with p52 (6) and enhance MHC class I presentation (23) indicating this hetero-complex is critical for triggering the expression of genes essential to up-regulate the cross-priming machinery in DCs.

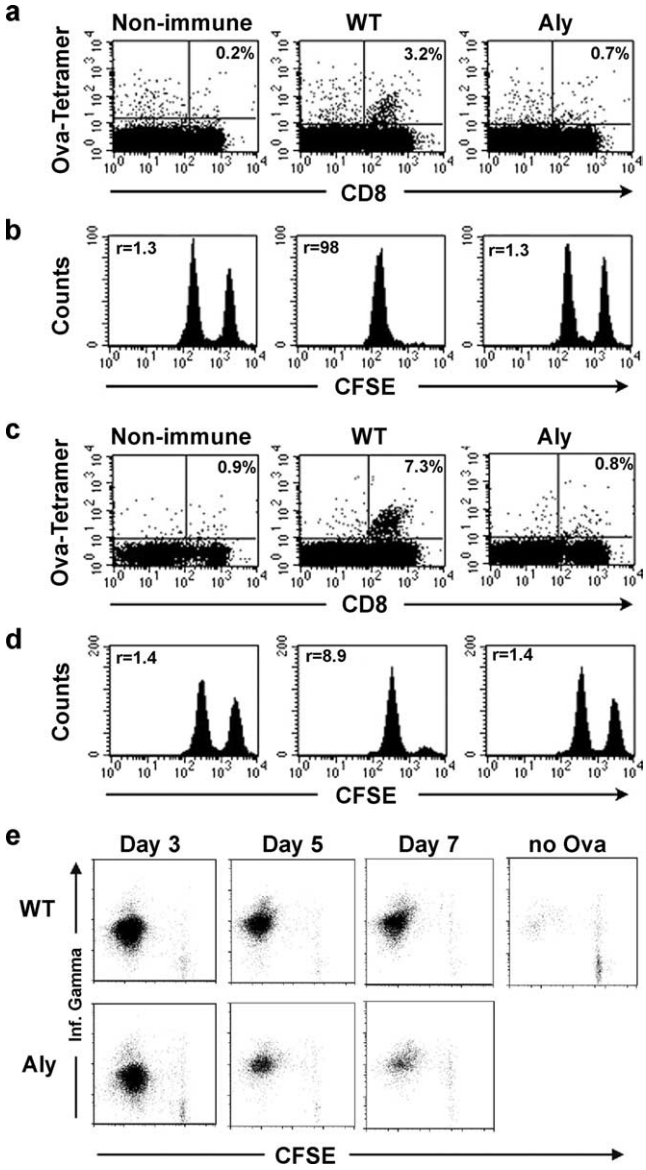

FIGURE 3. Aly mice do not cross-prime endogenous Ag-specific $CD8^+$ T cell responses, but MHC class II presentation appears intact. *a* and *b*, Mice were treated with anti-CD40 agonistic Ab, 1 mg of whole OVA protein and 50 μg LPS (*a*) or TLR7 agonist (*c*, *d*). Six days after treatment, spleens were isolated and analyzed for Ag-specific expansion by anti-CD8 and OVA MHC class I tetramer (*top panels*). Numbers in top right quadrant represent the percentage of $CD8^+$ cells that are OVA-specific. On day 5 after treatment, mice were injected with B6 splenocytes loaded with OVA peptide (higher peak) as targets for in vivo cytolysis, or left unpulsed as internal specificity controls (lower peak). Data shown are representative of three experiments $n = 3$ mice per group. *e*, Mice (WT or Aly) received 1×10^6 $CD4^+$ OT2 OVA-specific TCR transgenic T cells that were CFSE labeled. 24 h later mice were treated with 2 mg of whole OVA protein and 25 μg of LPS. On indicated days, spleen cells were isolated and division of OT2 and IFN-γ production was assessed by gating on CD45.1+ and $CD4^+$ cells. Data typical of two experiments, four mice per group.

The observation that the Aly mutation results in defective cross-priming in vivo raised the possibility that the Aly mouse may have broad defects in their ability to prime T cells. To test this, we verified the ability of the Aly mouse to prime a naive $CD4^+$ T cell

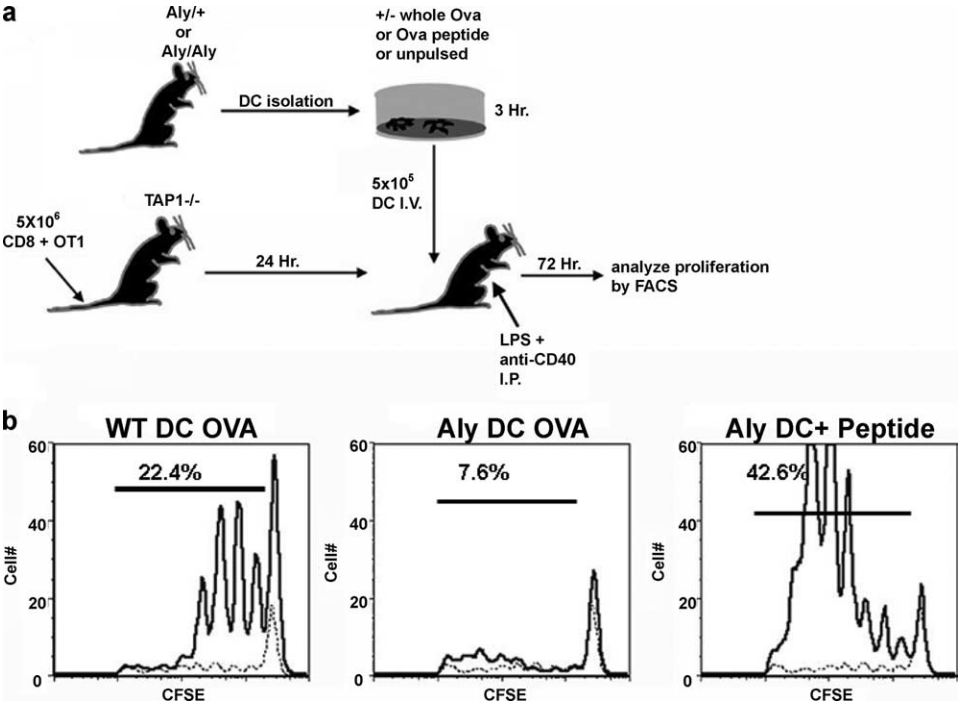

FIGURE 4. Cross-priming defects seen in Aly mouse are not due to defective environment. *a*, Schematic diagram of transfers performed in data shown in Fig. 4. *b*, OT1 expansion in TAP1−/− mice that received either WT (*left panel*) or Aly DCs (*middle*) pulsed with whole OVA protein. Histograms show OT1 expansion in TAP1−/− mice gating on $CD8^+$ and MHC class I tetramer OVA binding. Right panel shows TAP1−/− mice that received Aly DCs pulsed with OVA peptide. Dotted lines in each panel represent OT1 expansion in TAP1−/− mice that received unpulsed DCs as a negative control. Numbers indicate the percent of cells divided minus the percent of no Ag control. Data represents three experiments, $n = 3$ mice per group.

response. Either WT or Aly mice received OVA-specific OT2 TCR transgenic $CD4^+$ T cells and were then immunized with whole OVA and LPS. The ability of Aly mice to prime a $CD4^+$ T cell response was evaluated in groups of mice over 3, 5, and 7 days post OVA injection. As can be seen in Fig. 3*e*, both the WT and Aly mice can prime $CD4^+$ T cell response as visualized by proliferation of the OT2 population (CFSE dilution) and IFN-γ production. Although the low threshold for priming high affinity OT2 cells may mask minor defects in MHC class II processing in the Aly mice, this observation indicates that functional NIK is involved in cross-presentation specifically and not the general function of DCs in Ag presentation, and specifically in MHC class II presentation.

Defects in cross-priming are not due to structural defects in the Aly mouse

In some cases, the profound immunodeficiency in Aly mice has been attributed solely to the lack of lymph nodes and organized structures in other secondary lymphoid organs (24, 25). Clearly, disrupted architecture could impose a profound impact on DC function and the clonal expansion of Ag-reactive T cells. To selectively restore lymph node and secondary lymphoid organ architecture, but retain the Aly mutation in the DC compartment, purified DC^{Aly} or DC^{WT} were transferred into $TAP1^{-/-}$ hosts and their ability to cross-prime $CD8^+$ T cells in vivo was assessed. Briefly, isolated $CD11c^+$ splenic DCs were pulsed for 3 h in vitro with whole OVA protein and then were transferred i.v. into $TAP1^{-/-}$ mice. The recipients received CFSE-labeled $CD8^+$ purified OVA-specific OTI cells 24 h earlier. All mice received LPS and agonistic anti-CD40 i.p. at the time of DC transfer to induce DC maturation. $TAP1^{-/-}$ mice were used as recipients to limit presentation of OVA peptides to the adoptively transferred DCs (experimental layout depicted in Fig. 4*a*). In mice receiving DC^{WT}, cross-priming occurred and could be observed as dilution of CFSE in the OTI population (Fig. 4*b*). In mice that received DC^{Aly}, no cross-presentation was observed. Interestingly, if DC^{Aly} were pulsed with OVA peptide, thus eliminating the requirement of uptake and processing, they induced robust priming and expansion of the OTI cells. This indicates that the DC^{Aly} cells do not lack MHC class I or costimulatory molecules required to prime $CD8^+$ T cells, and migrate to the appropriate subanatomical sites in vivo to drive CD8 responses. However, DC^{Aly} have a profound and specific defect in processing whole Ags in the cross-priming pathway.

Cross-priming defects seen in the Aly mouse are DC intrinsic

The findings that DC^{Aly} cannot mediate cross-priming when transferred into an intact recipient strongly suggests an intrinsic defect in DC function. To confirm an intrinsic defect in DC^{Aly} cross-priming their ability to cross-prime was evaluated in vitro. Purified $CD11c^+$ splenic DCs were cultured with $CD8^+$ CFSE-labeled OTI TCR transgenic T cells. Agonistic anti-CD40 Ab, LPS and decreasing concentrations of whole OVA protein were added to the cultures to mature the DCs and induce cross-presentation. As seen in Fig. 5*a*, OVA is efficiently cross-presented by DC^{WT} at ranges of OVA from 12.5 to 1.25 μg/ml. In contrast, there is a dramatic shift in the dose response to OVA protein using DC^{Aly}.

An alternative means to assess cross-presentation efficiency of DCs is to measure the activation of a MHC class I-restricted, OVA-specific T cell hybridoma. Upon recognition of OVA peptide-MHC class I, this cell line produces IL-2 (26). One advantage of this system is that the production of IL-2 is independent of the costimulatory activities of the DCs and IL-2 is correlated with the density of MHC class I-restricted Ag on the surface of the APC (27). DCs were cultured with the CD8OVA hybridoma (Fig. 5*b*) and the amount of IL-2 produced was quantified (26). In conditions identical to those used in Fig. 5*a*, the production of IL-2 by cultures containing DC^{WT} was greater than those with DC^{Aly}. At 12.5 μg/ml OVA protein, DC^{Aly} induced 50% the production of IL-2 when compared with DC^{WT}. At the lower doses of OVA, DC^{Aly} were unable to induce IL-2 production while the DC^{WT} still induced detectable production of IL-2.

Cross-priming represents a series of complex events that culminate in the presentation of MHC class I-binding proteins on the DC surface. Defects in cross-priming seen in RelB−/− DCs has been attributed to a reduced ability to take up Ags (14). To test whether

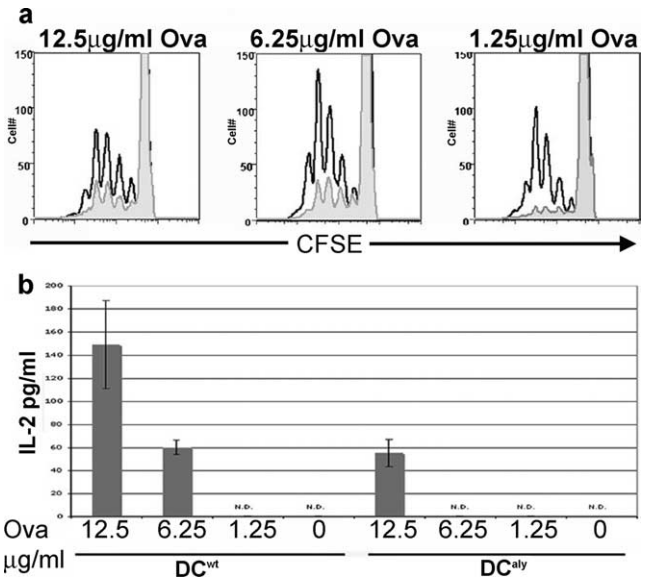

FIGURE 5. Defects seen in Aly DC are cell-intrinsic. *a*, In vitro expansion of OT1 T cells to dilutions of whole OVA protein with either WT DCs (dark lines), or Aly DCs (shaded). DCs were purified from spleen by anti-CD11c magnetic beads. The OT1 cells were purified from spleen and lymph node by anti-CD8 magnetic beads. All wells contained LPS and anti-CD40 Ab to induce cross-presentation. DC to T cell ratio was 1:1. Data representative of two experiments, three wells per group. *b*, IL-2 production by CD8OVA T cell hybridoma in response to WT or Aly DC processing of whole OVA. Cells were cultured under similar conditions as described in (*a*). After 24 h of coculture supernatants were collected and IL-2 concentrations were quantitated by ELISA. Data shown for one of two identical experiments, $n = 3$ wells per group.

a similar defect is manifested in the DC^{Aly}, DC^{WT} and DC^{Aly} were cultured with Alexa Fluor 488-conjugated latex beads to evaluate phagocytosis or Alexa Fluor 488-conjugated AcLDL to quantify receptor-mediated endocytosis. As shown in Fig. 6*a*, there is no apparent difference in phagocytic ability or receptor-mediated endocytosis. Further, no defect was seen in the Aly DCs ability to take up soluble OVA as tested by exposing purified DCs from Aly or WT mice to OVA protein conjugated to Alexa Fluor 488 either in vitro or in vivo (Fig. 6, *b* and *c*, respectively). To test whether Aly DCs have a defect in processing Ag, we incubated purified splenic DCs from WT or Aly mice with DQ-OVA. DQ-OVA is OVA protein conjugated with a fluorophore in such a way that the signal is quenched in the whole OVA form. As OVA is processed and broken down, the fluorophore becomes un-quenched and can be visualized by flow cytometry. Fig. 6*d*, *top panel*, shows the signal developed as DC^{WT} (*right*) or DC^{Aly} (*left*) process DQ-OVA after 6 h of incubation at 37°C. In Fig. 6*d*, *bottom panel*, signals from Aly or WT DCs are overlaid, and as can be seen, there appears to be no difference between the Aly or WT DCs ability to process Ag in this system.

DC^{Aly} migrate normally in vivo after TLR/CD40 signaling

Migration and survival are key elements in the ability of DCs to mediate the initiation of cell-mediated immunity (CMI). TLR signaling is known to trigger DC migration. After TLR signaling, DC down-regulate CCR2 and up-regulate CCR7 and migrate to CCL19/CCL21 in the PALS where they can interact with naive T cells. Once resituated in the PALS, prosurvival cues from T cells through CD40 or TRANCE induce heightened DC longevity. In the absence of these signals, DCs are rapidly cleared by apoptosis. Previous studies have found that Aly mice have reduced levels of CCL19/CCL21 (28), providing justification to study defects in DC migration. Because an inability to migrate appropriately to these cytokines would globally impact on the development of CMI in mice (29, 30), studies were executed to evaluate the ability of DC^{Aly} to traffic to defined histological sites following triggering with TLR agonists in vivo.

First, the ability of DCs from the WT and Aly mouse to regulate the expression of chemokine receptors and respond to migratory chemokines in vivo was evaluated. LPS and anti-CD40 were administered to Aly or WT mice and the expression of CCR2 and CCR7 was determined. After 6 h, DCs were isolated from the mice and real-time RT-PCR was performed to quantify the expression of CCR2, which is present on immature DCs and CCR7, which is up-regulated during TLR-induced maturation (31). As can be seen in Fig. 7*a*, in vivo LPS treatment resulted in down-regulation of CCR2 and up-regulation of CCR7 in both the DC^{Aly} and the DC^{WT}. Next, the impact of CD40 and/or TLR triggering on the migration of DCs in WT and Aly mice in vivo was determined. In untreated WT mouse spleen, the majority of DCs seen are in the marginal zones and the bridging zones between B cell follicles (Fig. 7*b*, *top*). Although the Aly mouse lacks defined B cell follicles, the general arrangement of the T cell area and DC localization appears normal. Six hours after systemic treatment with LPS, the DCs have migrated to the PALS in both the WT and the Aly mice indicating that the migration of DCs after TLR-induced maturation appears normal in the Aly mouse (Fig. 7*b*, *bottom*).

Genes regulated by the NF-κB2 pathway in DC

The findings thus far illustrate that the NF-κB2 pathway in DCs is not involved in early changes in costimulatory molecule expression, chemokine and cytokine production, the up-regulation of chemokine receptors or MHC class II-dependent presentation. However, this pathway is critical for the in vivo survival of matured DCs, and the ability of those DC to cross-present Ag to $CD8^+$ T cells. To gain a more global perspective on genes that are regulated in DCs in vivo by the NF-κB2 pathway, transcriptional profiling of in vivo activated DCs was pursued. Fig. 8 summarizes several new targets of interest that were found in our screen for NF-κB2 regulated genes in DCs. Several of these targets have clear implications in the survival defect seen after maturation, for example induction of c-Flip, which has been shown to be an anti-apoptotic mechanism of DC survival induced by CD40 signaling (32). Likewise, serpinb9 (spi6) has been shown to protect cells from granzyme B-mediated killing. Spi6 has been shown to be increased in DCs specifically after CD40 engagement, thus making DCs resistant to $CD8^+$ T cell-mediated killing during presentation of Ags (33). These two genes indicate possible escape mechanisms from T cell-mediated killing afforded via CD40 signaling. In a recent report, regulatory T cells were shown to kill target cells via granzyme B (34). It is thus possible to speculate that one mechanism of tolerance maintenance used by T regulatory cells may be to kill inappropriately matured DCs presenting self-Ag and that CD40 signaling may rescue such DCs from clearance in a similar way to what we have observed in Fig. 7. IL-15 and IL-15R likewise are genes that appear to be regulated by NIK. IL-15 has recently been shown to act as a survival factor for DCs after maturation (35). Genes involved in Ag processing and presentation were observed to be deficient after maturation of the Aly DCs. We observed several genes including cathepsin E, Lamp1, and the proteosome subunit 26s and others (see Fig. 8, *bottom group*). Quite interestingly, cathepsin E has been implicated in endosomal degradation of proteins (36) and thus may be partially responsible for our Ag-processing observations. Lamp1 is commonly used as a

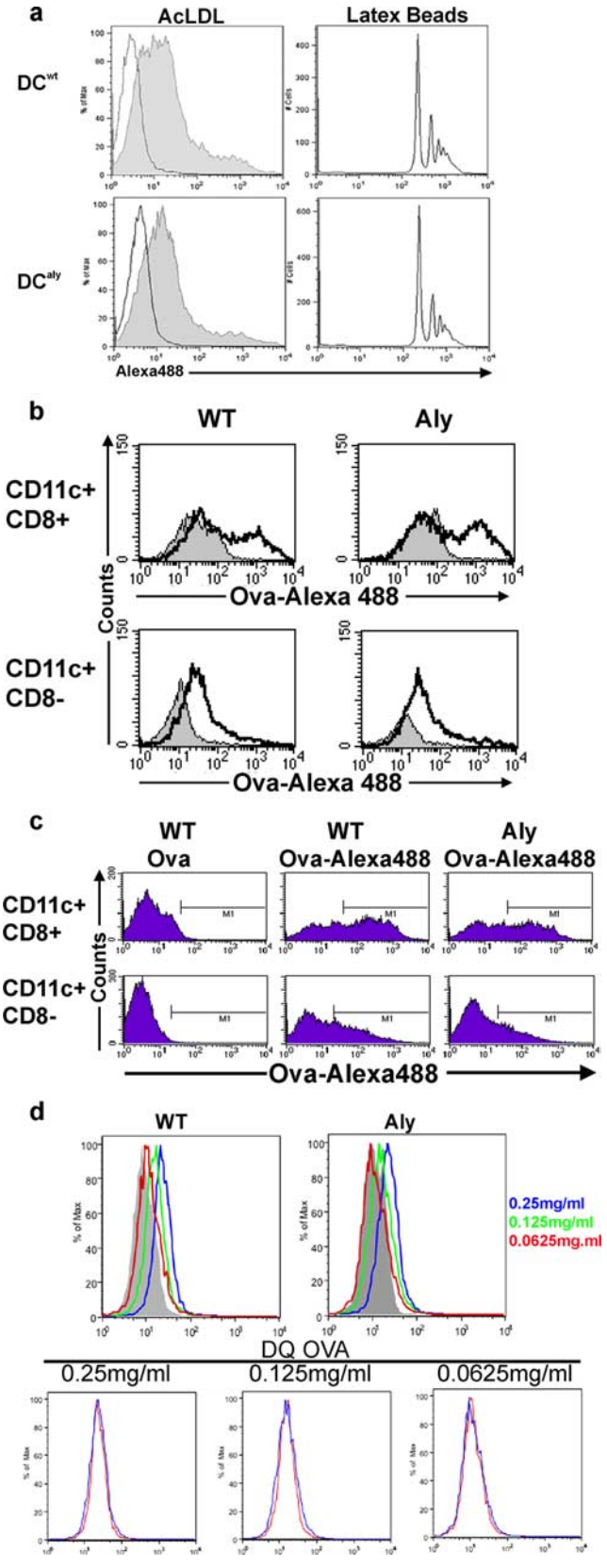

FIGURE 6. Ag uptake and processing appear normal in Aly DCs. *a*, Receptor-mediated endocytosis and phagocytosis in WT DCs compared with Aly DCs. CD11c+ splenic DCs from WT (*top panels*) or Aly mice were cultured for 2 h at 37°C with AcLDL or latex beads both conjugated to Alexa Fluor 488. *Left panel* shows AcLDL uptake, shaded histograms represent DCs incubated with AcLDL, empty histograms are untreated DCs. Data representative of three experiments $n = 3$ wells per group. *b*, OVA uptake by Aly DCs is not impaired. Splenic DCs from WT or Aly mice were incubated for 2.5 h in vitro with OVA-Alexa Fluor 488 at either 4°C (shaded) or 37°C (unshaded). OVA uptake was measured in both the CD11c+ $CD8^+$ DC population (*top panel*) and the CD11c+ $CD8^-$ population (*bottom panel*). Data is representative of 2 separate experiments. *c*, In vivo uptake of OVA protein is normal in Aly mice. WT or Aly mice were injected i.v. with either unlabeled OVA (*left panel*) or Alexa Fluor 488 conjugated OVA (*right panels*). After 24 h, spleen cells were isolated and OVA uptake was measured by FACS. OVA-Alexa Fluor 488 uptake was measured in CD11c+ $CD8^+$ (*top row*) or CD11c+ $CD8^-$ (*bottom row*) subpopulations. Data shown is representative of observations in two separate experiments. *d*, Ag processing by DCs. Purified splenic Aly or WT DCs were incubated with DQ-OVA for 6 h in vitro. Ag processing was visualized as un-quenching of DQ-OVA and subsequent fluorescence. Top panel shows dilutions of DQ-OVA and processing by WT (*left*) or Aly DCs (*right*) gray histogram shows signal from DCs incubated with 0.25 μg/ml DQ-OVA and incubated on ice to account for background fluorescence. The bottom panel overlays DQ-OVA signals of WT (blue) or Aly (red) for each dilution tested. Data representative of two experiments triplicate wells per dilution.

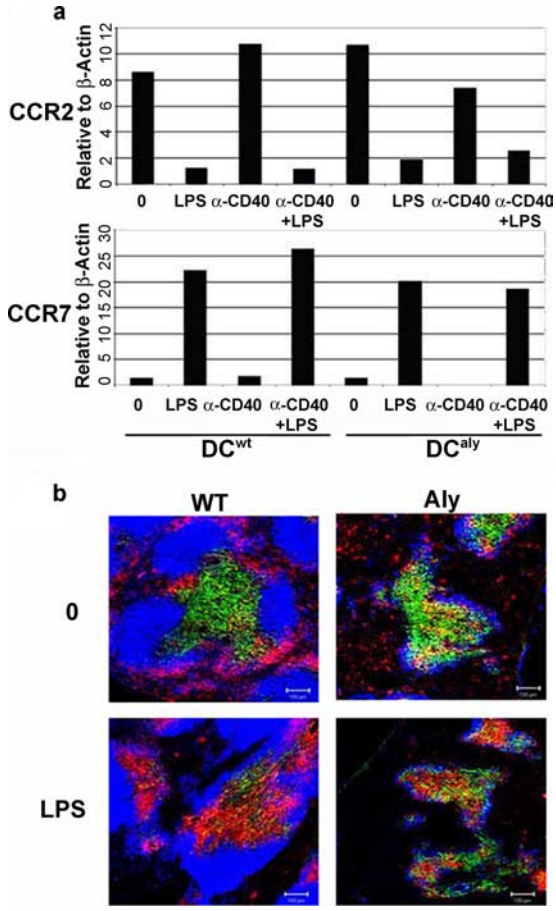

FIGURE 7. Defects observed in the Aly mouse are not due to structural defects in the spleen. *a*, Real-time RT-PCR for chemokine receptor expression after in vivo maturation in Aly or WT mice. Mice were treated with either LPS or agonistic anti-CD40 Ab or both for 6 h. DCs were then isolated from spleen and RNA was extracted and subject to reverse transcription. Signals were amplified with primers specific for CCR2 or CCR7. Data is represented as relative to β-actin expression. *b*, Migration of Aly DCs is normal in vivo. Mice were treated with LPS for 6 h. Spleens were isolated, sectioned and stained with Abs recognizing B cells (B220) in blue, T cells (CD4) green, and DCs (CD11c) in red. Images represent similar results seen in three experiments, $n = 3$ mice per group. Scale bar = 100 mm.

lysosomal marker and has recently been shown to have a functional role in phagosome to lysosome fusion (37) a function that may play a role in processing of exogenously acquired proteins. In

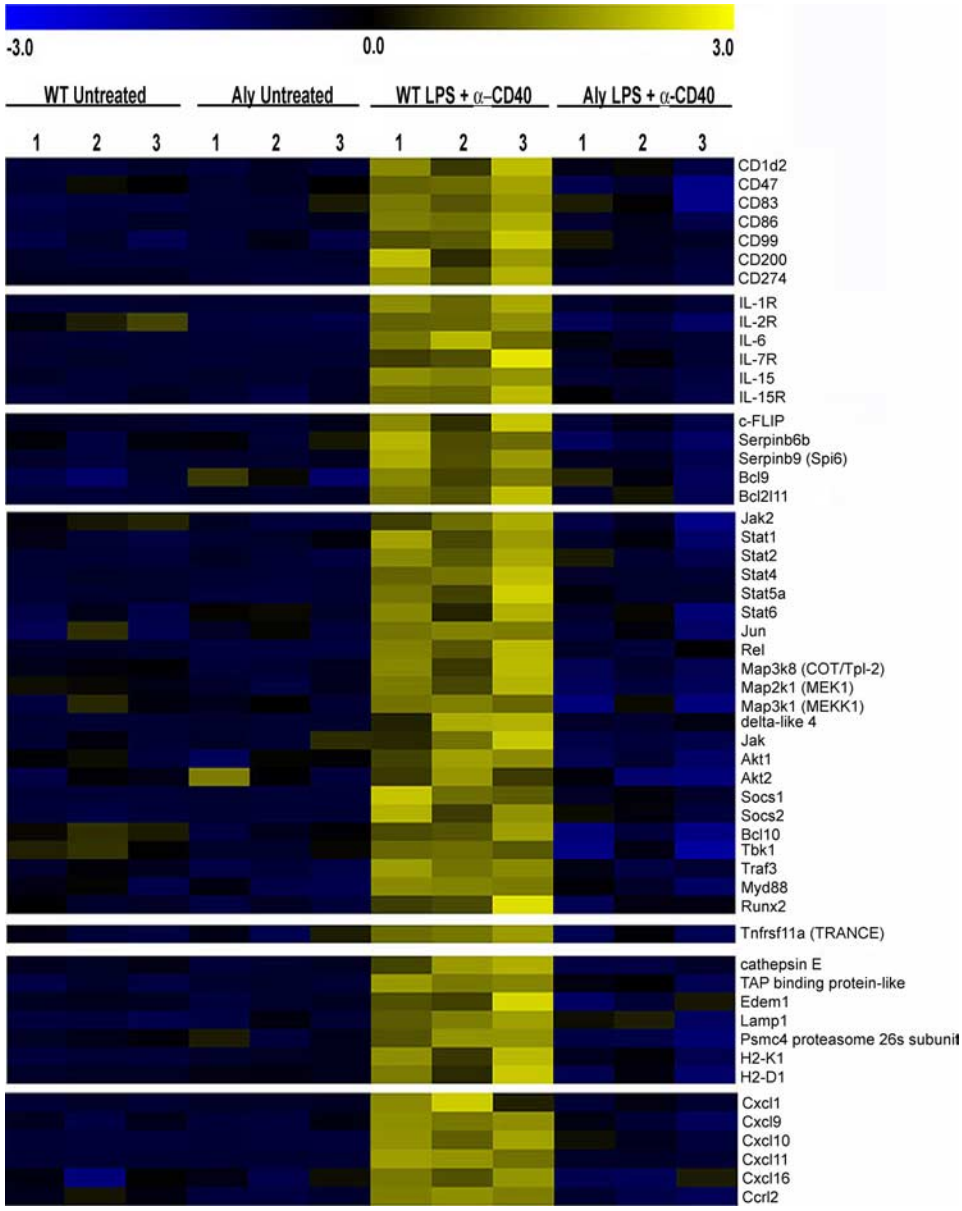

FIGURE 8. Expression profiles of NIK/NF-κB2 responsive genes in DCs matured in vivo. WT or Aly mice were treated for 6 h with LPS and anti-CD40 Ab. After treatment spleens were isolated digested with DNase and Liberase and purified by magnetic anti-CD11c beads followed by sorting by FACS to increase purity to greater than 95%. RNA was amplified and hybridized to Affymetrix 430.2 whole mouse genome expression arrays. Genes shown represent a small subset of genes where mRNA was up-regulated by TLR/CD40 treatment in the WT but not the Aly samples. Heat map represents standardized data graphed on a relative scale.

the analysis performed here, the fact that the entire list of genes up-regulated in the DC^{WT} but not in the DC^{Aly} numbers 916 indicated that the scope of genes regulated by NIK/NF-κB2 in DCs may be much greater than previously thought. This indicates that the defects in cross-priming $CD8^+$ T cells to soluble Ag seen in DCs from Aly mice are due to a complex matrix of gene transcription defects.

Discussion

The Aly mouse has been used extensively as a model of a "lymph node-less" mouse whose immune responses are impaired solely due to the lack of the appropriate immune architecture (9, 24, 25, 38, 39). The data reported herein show that DCs in the Aly mice have significant intrinsic defects in cross-presentation, which contributes significantly to the immune incompetence of this mutant mouse. The data show that the NF-κB2 pathway in DCs is not involved in early changes in costimulatory molecule expression (as seen in Fig. 2), or the up-regulation of chemokine receptors (as seen in Fig. 7) and MHC class II presentation. Hence, many of the early events in DC maturation are intact.

Initially, when mutations in NIK were discovered, it was believed that pathways involving NIK signaling were restricted to genes involved in lymph node development. It soon became clear, however, that this pathway was also involved in B cell (24, 40) and T cell function (41). The work presented here investigates the role of this pathway in APC function and show that the NIK and the NF-κB2 pathway exert specific effects on DC function. Further, we report for the first time the pattern of genes regulated by the p52 transcription factor in DCs via whole genome transcriptional analysis.

The important role for NIK in cross-priming $CD8^+$ T cell responses is a novel finding that further defines the mechanistic role of CD40 in APC function. Several earlier studies on other cell types have shown that NIK is required for activation of the NF-κB2 pathway, and activation induces the release of p52/RelB dimers for transcription. As one might expect, other mutations in this pathway also result in deficiencies similar to those observed in RelB-deficient mice. In fact, mice that lack the NF-κB family member RelB have been clearly shown to have defects in cross-priming (13, 14). These studies also revealed a defect in classical

priming of T cells from RelB−/− mice indicating that a lack of individual transcription factors in this pathway may result in multiple defects. Recently it has been shown that DCs deficient in NF-κB2 are hyperactive in cytokine production and in ability to prime naive $CD4^+$ T cells (15). This phenotype is due to constitutive RelB nuclear translocation and thus is not contradictory to our findings that blockade of normal p52/RelB system results in defects in DC function.

Cross-priming of $CD8^+$ T cells is classically defined as functional expansion of CTLs to cell-associated Ags. In our model, however, we have chosen to study the ability of soluble Ags to prime a functional $CD8^+$ T cell response, and thus this model does not meet the classical definition of the term "cross-priming" as historically defined (42, 43). However, the ability to prime a $CD8^+$ T cell response to soluble Ags as studied in our system has great potential and clinical application when attempting to induce a functional response in the case of tumor vaccine strategies.

The pattern of genes activated by the NF-κB2 pathway have been studied in response to lymphotoxin stimuli in fibroblasts (6), but until now the pattern of genes regulated by this pathway has not been investigated in DC after CD40 activation. Analysis of gene arrays hybridized using RNA from purified DCs matured in vivo gives us the added advantage of allowing investigation of genes regulated during DC maturation in their normal environment. Our studies indicate that NIK and the NF-κB2 signaling pathway have critical and previously un-described functions in cross-priming mechanisms. The data presented here contributes further mechanistic explanations of how downstream signaling events through CD40 in DC results in enhanced adaptive T cell responses seen after administration of agonistic anti-CD40 Abs. This data also begins to study the genes regulated by NIK/NF-κB2 in hematopoietic cells, and such knowledge may aid in developing new strategies for both inducing tolerance in cases of autoimmunity and intentionally breaking self-tolerance in tumor vaccine strategies.

Acknowledgments

We thank Leo LeFrancois and Steven Ley for Abs.

Disclosures

The authors have no financial conflict of interest.

References

1. Malinin, N. L., M. P. Boldin, A. V. KOVAlenko, and D. Wallach. 1997. MAP3K-related kinase involved in NF-κB induction by TNF, CD95, and IL-1. *Nature* 385: 540–544.
2. Yin, L., L. Wu, H. Wesche, C. D. Arthur, J. M. White, D. V. Goeddel, and R. D. Schreiber. 2001. Defective lymphotoxin-β receptor-induced NF-κB transcriptional activity in NIK-deficient mice. *Science* 291: 2162–2165.
3. Senftleben, U., Y. Cao, G. Xiao, F. R. Greten, G. Krahn, G. Bonizzi, Y. Chen, Y. Hu, A. Fong, S. C. Sun, and M. Karin. 2001. Activation by IKKα of a second, evolutionary conserved, NF-κB signaling pathway. *Science* 293: 1495–1499.
4. Xiao, G., E. W. Harhaj, and S. C. Sun. 2001. NF-κ-inducing kinase regulates the processing of NF-κB2 p100. *Mol. Cell.* 7: 401–409.
5. Xiao, G., A. Fong, and S. C. Sun. 2004. Induction of p100 processing by NF-κB-inducing kinase involves docking IκB kinase α (IKKα) to p100 and IKKα-mediated phosphorylation. *J. Biol. Chem.* 279: 30099–30105.
6. Dejardin, E., N. M. Droin, M. Delhase, E. Haas, Y. Cao, C. Makris, Z. W. Li, M. Karin, C. F. Ware, and D. R. Green. 2002. The lymphotoxin-β receptor induces different patterns of gene expression via two NF-κB pathways. *Immunity* 17: 525–535.
7. Claudio, E., K. Brown, S. Park, H. Wang, and U. Siebenlist. 2002. BAFF-induced NEMO-independent processing of NF-κB2 in maturing B cells. *Nat. Immunol.* 3: 958–965.
8. Coope, H. J., P. G. Atkinson, B. Huhse, M. Belich, J. Janzen, M. J. Holman, G. G. Klaus, L. H. Johnston, and S. C. Ley. 2002. CD40 regulates the processing of NF-κB2 p100 to p52. *EMBO J.* 21: 5375–5385.
9. Miyawaki, S., Y. Nakamura, H. Suzuka, M. Koba, R. Yasumizu, S. Ikehara, and Y. Shibata. 1994. A new mutation, aly, that induces a generalized lack of lymph nodes accompanied by immunodeficiency in mice. *Eur. J. Immunol.* 24: 429–434.
10. Matsushima, A., T. Kaisho, P. D. Rennert, H. Nakano, K. Kurosawa, D. Uchida, K. Takeda, S. Akira, and M. Matsumoto. 2001. Essential role of nuclear factor (NF)-κB-inducing kinase and inhibitor of κB (IκB) kinase α in NF-κB activation through lymphotoxin β receptor, but not through tumor necrosis factor receptor I. *J. Exp. Med.* 193: 631–636.
11. Shinkura, R., K. Kitada, F. Matsuda, K. Tashiro, K. Ikuta, M. Suzuki, K. Kogishi, T. Serikawa, and T. Honjo. 1999. Alymphoplasia is caused by a point mutation in the mouse gene encoding Nf-κb-inducing kinase. *Nat. Genet.* 22: 74–77.
12. Luftig, M. A., E. Cahir-McFarland, G. Mosialos, and E. Kieff. 2001. Effects of the NIK aly mutation on NF-κB activation by the Epstein-Barr virus latent infection membrane protein, lymphotoxin β receptor, and CD40. *J. Biol. Chem.* 276: 14602–14606.
13. Zanetti, M., P. Castiglioni, S. Schoenberger, and M. Gerloni. 2003. The role of relB in regulating the adaptive immune response. *Ann. NY Acad. Sci.* 987: 249–257.
14. Castiglioni, P., E. M. Janssen, K. R. Prilliman, M. Gerloni, S. Schoenberger, and M. Zanetti. 2002. Cross-priming is under control of the relB gene. *Scand. J. Immunol.* 56: 219–223.
15. Speirs, K., L. Lieberman, J. Caamano, C. A. Hunter, and P. Scott. 2004. Cutting edge: NF-κB2 is a negative regulator of dendritic cell function. *J. Immunol.* 172: 752–756.
16. O'Keeffe, M., R. J. Grumont, H. Hochrein, M. Fuchsberger, R. Gugasyan, D. Vremec, K. Shortman, and S. Gerondakis. 2005. Distinct roles for the NF-κB1 and c-Rel transcription factors in the differentiation and survival of plasmacytoid and conventional dendritic cells activated by TLR-9 signals. *Blood* 106: 3457–3464.
17. Ouaaz, F., J. Arron, Y. Zheng, Y. Choi, and A. A. Beg. 2002. Dendritic cell development and survival require distinct NF-κB subunits. *Immunity* 16: 257–270.
18. Ahonen, C. L., C. L. Doxsee, S. M. McGurran, T. R. Riter, W. F. Wade, R. J. Barth, J. P. Vasilakos, R. J. Noelle, and R. M. Kedl. 2004. Combined TLR and CD40 triggering induces potent $CD8^+$ T cell expansion with variable dependence on type I IFN. *J. Exp. Med.* 199: 775–784.
19. Wu, L., A. D'Amico, K. D. Winkel, M. Suter, D. Lo, and K. Shortman. 1998. RelB is essential for the development of myeloid-related $CD8\alpha^-$ dendritic cells but not of lymphoid-related $CD8\alpha^+$ dendritic cells. *Immunity* 9: 839–847.
20. Dudziak, D., A. O. Kamphorst, G. F. Heidkamp, V. R. Buchholz, C. Trumpfheller, S. Yamazaki, C. Cheong, K. Liu, H. W. Lee, C. G. Park, et al. 2007. Differential antigen processing by dendritic cell subsets in vivo. *Science* 315: 107–111.
21. del Rio, M. L., J. I. Rodriguez-Barbosa, E. Kremmer, and R. Forster. 2007. $CD103^-$ and $CD103^+$ bronchial lymph node dendritic cells are specialized in presenting and cross-presenting innocuous antigen to $CD4^+$ and $CD8^+$ T cells. *J. Immunol.* 178: 6861–6866.
22. Yanagawa, Y., and K. Onoe. 2006. Distinct regulation of CD40-mediated interleukin-6 and interleukin-12 productions via mitogen-activated protein kinase and nuclear factor κB-inducing kinase in mature dendritic cells. *Immunology* 117: 526–535.
23. O'Sullivan, B. J., K. P. MacDonald, A. R. Pettit, and R. Thomas. 2000. RelB nuclear translocation regulates B cell MHC molecule, CD40 expression, and antigen-presenting cell function. *Proc. Natl. Acad. Sci. USA* 97: 11421–11426.
24. Karrer, U., A. Althage, B. Odermatt, H. Hengartner, and R. M. Zinkernagel. 2000. Immunodeficiency of alymphoplasia mice (aly/aly) in vivo: structural defect of secondary lymphoid organs and functional B cell defect. *Eur. J. Immunol.* 30: 2799–2807.
25. Karrer, U., A. Althage, B. Odermatt, C. W. Roberts, S. J. Korsmeyer, S. Miyawaki, H. Hengartner, and R. M. Zinkernagel. 1997. On the key role of secondary lymphoid organs in antiviral immune responses studied in alymphoplastic (aly/aly) and spleenless ($Hox11^{-/-}$ mutant mice. *J. Exp. Med.* 185: 2157–2170.
26. Pfeifer, J. D., M. J. Wick, R. L. Roberts, K. Findlay, S. J. Normark, and C. V. Harding. 1993. Phagocytic processing of bacterial antigens for class I MHC presentation to T cells. *Nature* 361: 359–362.
27. Potter, N. S., and C. V. Harding. 2001. Neutrophils process exogenous bacteria via an alternate class I MHC processing pathway for presentation of peptides to T lymphocytes. *J. Immunol.* 167: 2538–2546.
28. Fagarasan, S., R. Shinkura, T. Kamata, F. Nogaki, K. Ikuta, K. Tashiro, and T. Honjo. 2000. Alymphoplasia (aly)-type nuclear factor κB-inducing kinase (NIK) causes defects in secondary lymphoid tissue chemokine receptor signaling and homing of peritoneal cells to the gut-associated lymphatic tissue system. *J. Exp. Med.* 191: 1477–1486.
29. Martin-Fontecha, A., S. Sebastiani, U. E. Hopken, M. Uguccioni, M. Lipp, A. Lanzavecchia, and F. Sallusto. 2003. Regulation of dendritic cell migration to the draining lymph node: impact on T lymphocyte traffic and priming. *J. Exp. Med.* 198: 615–621.
30. Hopken, U. E., J. Droese, J. P. Li, J. Joergensen, D. Breitfeld, H. G. Zerwes, and M. Lipp. 2004. The chemokine receptor CCR7 controls lymph node-dependent cytotoxic T cell priming in alloimmune responses. *Eur. J. Immunol.* 34: 461–470.
31. Sallusto, F., P. Schaerli, P. Loetscher, C. Schaniel, D. Lenig, C. R. Mackay, S. Qin, and A. Lanzavecchia. 1998. Rapid and coordinated switch in chemokine receptor expression during dendritic cell maturation. *Eur. J. Immunol.* 28: 2760–2769.

32. Kreuz, S., D. Siegmund, P. Scheurich, and H. Wajant. 2001. NF-κB inducers upregulate cFLIP, a cycloheximide-sensitive inhibitor of death receptor signaling. *Mol. Cell. Biol.* 21: 3964–3973.
33. Medema, J. P., D. H. Schuurhuis, D. Rea, J. van Tongeren, J. de Jong, S. A. Bres, S. Laban, R. E. Toes, M. Toebes, T. N. Schumacher, et al. 2001. Expression of the serpin serine protease inhibitor 6 protects dendritic cells from cytotoxic T lymphocyte-induced apoptosis: differential modulation by T helper type 1 and type 2 cells. *J. Exp. Med.* 194: 657–667.
34. Gondek, D. C., L. F. Lu, S. A. Quezada, S. Sakaguchi, and R. J. Noelle. 2005. Cutting edge: contact-mediated suppression by $CD4^+CD25^+$ regulatory cells involves a granzyme B-dependent, perforin-independent mechanism. *J. Immunol.* 174: 1783–1786.
35. Dubois, S. P., T. A. Waldmann, and J. R. Muller. 2005. Survival adjustment of mature dendritic cells by IL-15. *Proc. Natl. Acad. Sci. USA* 102: 8662–8667.
36. Kakehashi, H., T. Nishioku, T. Tsukuba, T. Kadowaki, S. Nakamura, and K. Yamamoto. 2007. Differential regulation of the nature and functions of dendritic cells and macrophages by cathepsin E. *J. Immunol.* 179: 5728–5737.
37. Huynh, K. K., E. L. Eskelinen, C. C. Scott, A. Malevanets, P. Saftig, and S. Grinstein. 2007. LAMP proteins are required for fusion of lysosomes with phagosomes. *EMBO J.* 26: 313–324.
38. Obhrai, J. S., M. H. Oberbarnscheidt, T. W. Hand, L. Diggs, G. Chalasani, and F. G. Lakkis. 2006. Effector T cell differentiation and memory T cell maintenance outside secondary lymphoid organs. *J. Immunol.* 176: 4051–4058.
39. Lakkis, F. G., A. Arakelov, B. T. Konieczny, and Y. Inoue. 2000. Immunologic "ignorance" of vascularized organ transplants in the absence of secondary lymphoid tissue. *Nat. Med.* 6: 686–688.
40. Garceau, N., Y. Kosaka, S. Masters, J. Hambor, R. Shinkura, T. Honjo, and R. J. Noelle. 2000. Lineage-restricted function of nuclear factor κB-inducing kinase (NIK) in transducing signals via CD40. *J. Exp. Med.* 191: 381–386.
41. Matsumoto, M., T. Yamada, S. K. Yoshinaga, T. Boone, T. Horan, S. Fujita, Y. Li, and T. Mitani. 2002. Essential role of NF-κB-inducing kinase in T cell activation through the TCR/CD3 pathway. *J. Immunol.* 169: 1151–1158.
42. Carbone, F. R., and M. J. Bevan. 1989. Induction of OVAlbumin-specific cytotoxic T cells by in vivo peptide immunization. *J. Exp. Med.* 169: 603–612.
43. Moore, M. W., F. R. Carbone, and M. J. Bevan. 1988. Introduction of soluble protein into the class I pathway of antigen processing and presentation. *Cell* 54: 777–785.